

Formation of an Exciton Polariton Condensate: Thermodynamic versus Kinetic Regimes

J. Kasprzak,^{1,2} D. D. Solnyshkov,³ R. André,¹ Le Si Dang,¹ and G. Malpuech³

¹CEA-CNRS Group "Nanophysique et Semiconducteurs," Institut Néel, CNRS et Université Joseph Fourier, BP 166, F-38042 Grenoble Cedex 9, France

²School of Physics and Astronomy, Cardiff University, Cardiff, CF24 3AA, United Kingdom

³LASMEA, CNRS, University Blaise Pascal, 24 avenue des Landais, 63177 Aubière cedex, France
(Received 18 April 2008; revised manuscript received 11 August 2008; published 1 October 2008)

We measure the polariton distribution function and the condensation threshold versus the photon-exciton detuning and the lattice temperature in a CdTe microcavity under nonresonant pumping. The results are reproduced by simulations using semiclassical Boltzmann equations. At negative detuning we find a kinetic condensation regime: the distribution is not thermal and the threshold is governed by the relaxation kinetics. At positive detuning, the distribution becomes thermal and the threshold is governed by the thermodynamic parameters of the system. Both regimes are a manifestation of polariton lasing, whereas only the latter is related to Bose-Einstein condensation defined as an equilibrium phase transition.

DOI: [10.1103/PhysRevLett.101.146404](https://doi.org/10.1103/PhysRevLett.101.146404)

PACS numbers: 71.36.+c, 78.67.-n

Microcavity exciton polaritons were observed experimentally in 1992 [1]. These quasiparticles arise from the strong coupling between the optical mode of a Fabry-Perot resonator and the excitonic resonance of a semiconductor quantum well (QW) [2]. They behave at low density as bosonic particles, retaining from their excitonic component an interacting behavior and from their photonic part a light effective mass ($\sim 5 \times 10^{-5}$ free electron mass) and a lifetime in the picosecond range. Imamoğlu first proposed in 1996 [3] to use these properties to make a new kind of laser without inversion, for which the driving force is not the stimulated emission of photons, but stimulated scattering of polaritons towards a condensate, which leaks out of the microcavity by spontaneously emitting coherent photons. This was a dual-sided concept. It can be interpreted as a new proposal for the realization of laser-type sources [4–7]. It can also be seen as an example of Bose-Einstein condensation (BEC) of quasiparticles in a solid state system [8–11]. The question of the interpretation of the recent experimental findings in terms of polariton lasing or in terms of BEC remains hot nowadays. The arguments for the first point of view are that the emission of coherent photons does not require thermal equilibration within the polariton Bose gas and that the thermodynamics usually is not the driving force of the condensate formation. The arguments supporting the second point of view are that in well-defined experimental situations, in spite of the short polariton lifetime, the relaxation kinetics can be fast enough to reach a steady state Bose distribution.

As a starting point, let us assume that polaritons have an infinite lifetime and are in thermal equilibrium with a lattice at temperature T_{lat} (thermodynamic limit). At a given critical density $n_c^0(T_{\text{lat}})$, the distribution function becomes singular in $k_{\parallel} = 0$, triggering the onset of a long range spatial coherence: a Bose condensate forms. Then one can adiabatically switch on the lifetime, keeping

it much longer than any relaxation process. A nonresonant pumping should be simultaneously introduced, in order to compensate the radiative losses. In this picture the condensate emits coherent photons and can be certainly called a polariton laser, if one is interested in fabricating a device. On the other hand, there is no doubt that the associated phase transition is the BEC of polaritons. With further reducing the polariton lifetime, the distribution will stay close to the thermal one, depending on the relaxation kinetics. An effective temperature $T_{\text{eff}} > T_{\text{lat}}$ can be defined, if the kinetics responsible for equilibration is fast enough. In that case, the polariton gas is in self-equilibrium, but not necessarily in equilibrium with the lattice. If the kinetics is too slow with respect to the lifetime, an effective temperature cannot be defined anymore. In both cases the system could be called metastable, in the sense that it is not in thermal equilibrium with the lattice. In the following, we choose to call metastable only the state which cannot be described at all by a temperature. However, above some critical density $n_c > n_c^0(T_{\text{lat}})$, the noncondensed state, metastable or not, becomes unstable and condensation takes place. Again the condensed state can be described by an effective temperature and can be considered as a thermodynamic equilibrium state (or not, depending on the kinetics). The kinetics is faster in the condensed regime because of the stimulated nature of some of the transitions, which makes the achievement of an equilibrium state easier than for an uncondensed state. A system which evolves from a metastable uncondensed to a metastable condensed state can hardly be described in the framework of BEC, and is only a polariton laser. On the other hand, a system which is characterized by an effective temperature both below and above the condensation threshold is directly related to BEC, and as shown below, the threshold density value is in that case directly linked with the critical thermodynamic density of the bosonic

phase transition. Finally, a third case can occur in a narrow range of parameters which is the transition from a metastable uncondensed phase towards a condensed phase characterized by a temperature. The threshold value in that case is controlled by the kinetics, but the driving force leading to condensation is the tendency of the system to leave a metastable state to reach the more favorable thermodynamic situation, which is for the system to be condensed. Such a phase transition can be related again to BEC because the state above threshold is thermalized. We propose to call the phase transition occurring in such a case *kinetically driven Bose condensation*.

In this Letter, we investigate the polariton distribution function under nonresonant optical excitation in a CdTe microcavity, exhibiting Rabi splitting of $\Omega = 26$ meV up to $T_{\text{lat}} \approx 100$ K. The sample detail and the experimental methods were described elsewhere (see Ref. [9] and references therein). We present a large set of new measurements together with corresponding theoretical calculations. We determine the polariton phase diagram showing the condensation threshold P_{th} tuning two independent parameters, which are the photon-exciton detuning δ and T_{lat} . We show that all the above-mentioned regimes are experimentally accessible.

The numerical simulations of polariton relaxation are performed using the semiclassical Boltzmann equation which describes the dynamics of polaritons along the lower polariton branch (including exciton reservoir): $\partial n_{\mathbf{k}}/\partial t = P_{\mathbf{k}} - \Gamma_{\mathbf{k}} n_{\mathbf{k}} - n_{\mathbf{k}} \sum_{\mathbf{k}'} W_{\mathbf{k} \rightarrow \mathbf{k}'} (n_{\mathbf{k}'} + 1) + (n_{\mathbf{k}} + 1) \sum_{\mathbf{k}'} W_{\mathbf{k}' \rightarrow \mathbf{k}} n_{\mathbf{k}'}$. In this equation $n_{\mathbf{k}}$ is the occupation number of a state with wave-vector \mathbf{k} , whereas $P_{\mathbf{k}}$ and $\Gamma_{\mathbf{k}} n_{\mathbf{k}}$ terms describe pumping and decay of particles. $W_{\mathbf{k} \rightarrow \mathbf{k}'}$ includes exciton-phonon scattering rates $W_{\mathbf{k} \rightarrow \mathbf{k}'}^{\text{ph}}$ and exciton-exciton contribution which depends on the polariton distribution function [2]: $\sum_{\mathbf{q}} W_{\mathbf{k} \rightarrow \mathbf{k}', \mathbf{q}}^{xx} n_{\mathbf{q}} (1 + n_{\mathbf{q} + \mathbf{k} - \mathbf{k}'})$, where $W_{\mathbf{k} \rightarrow \mathbf{k}', \mathbf{q}}^{xx}$ is the constant of exciton-exciton interaction for corresponding wave vectors.

The system is considered to have cylindrical symmetry, and scattering processes with all wave vectors are properly accounted for [12,13]. The polariton spin degree of freedom is neglected. We have taken the experimental values of cavity photon lifetime (1 ps), exciton inhomogeneous broadening (1 meV), and exciton lifetime (140 ps). We do not describe the exciton formation process from electron-hole pairs, a process which mainly takes place through the interaction with optical phonons. We rather assume the direct generation of a Boltzmann distribution of excitons in CdTe. The pumping term, replenishing excitons in all 16 QWs, therefore reads $P_{\mathbf{k}} = A x_{\mathbf{k}}^{\text{LP}} e^{(E_0^X - E_{\text{PH}}^0)/E_{\text{PH}}^0}$, where $x_{\mathbf{k}}^{\text{LP}}$ is the exciton fraction, E_0^X the bare exciton energy, E_{PH}^0 the lower polariton energy, and E_{PH}^0 is the optical phonon energy. A is a constant controlling the pumping intensity. To theoretically estimate the external pumping density of power P_{ext} providing a given density of excitons P per unit of time, we use the formula: $P_{\text{ext}} = PE_0/[\alpha(1 -$

$R)]$. P is obtained as an integral of $P_{\mathbf{k}}$ over the reciprocal space divided by $N_{\text{QW}} (= 16)$, $\alpha = 3\%$ is the QW absorption coefficient, whereas $R = 0.15$ is the reflectivity of the microcavity at the pump energy $E_0 = 1.76$ eV. We estimate that $P_{\text{ext}} \approx 1$ kW/cm² produces $\sim 10^{10}$ cm⁻² excitons per QW, from which only $\sim 5 \times 10^8$ cm⁻² form the polariton Bose gas at the BEC threshold.

Figure 1(a) shows the occupancy of the polariton states versus their energy (counted from the ground state) for $\delta = +6.8$ meV and at the fixed $P_{\text{ext}} \sim 1$ kW/cm². T_{lat} is varied from 5.3 to 40 K. Above $T_{\text{lat}} \approx 60$ K, the condensation threshold is too high and the strong coupling could be lost in the strong excitation regime. Figure 1(b) shows the result of the corresponding simulations. One can observe that for any T_{lat} both theoretical and experimental curves can be fitted with a Bose distribution function, which allows to extract an effective temperature T_{eff} . The experimental and theoretical values of $(T_{\text{eff}} - T_{\text{lat}})/T_{\text{lat}}$ versus T_{lat} are plotted in Fig. 1(c). T_{eff} is slightly larger than T_{lat} below 20 K, but the discrepancy becomes small at higher temperature, where the system becomes well described by its thermodynamic features. The increase of the ground state population and the decrease of T_{eff} when T_{lat} decreases demonstrate that the phase transition is induced more by thermodynamics than by kinetics. The transition observed is similar to the ideal BEC, where the system evolves from one equilibrium situation to another. These features are well reproduced by the theoretical calculations. We find that the relaxation kinetics at this positive

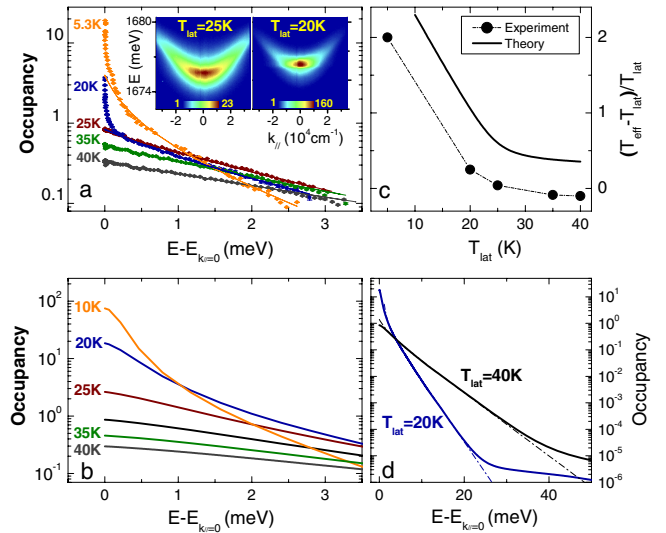


FIG. 1 (color online). (a) Experimental distributions of polaritons at different T_{lat} and at a constant pumping power close to threshold, $\delta = +6.8$ meV $= +0.26 \Omega$. Inset: measured polariton dispersion $E(k_{\parallel})$ in PL, logarithmic color scale. (b) Calculated distributions of polaritons under the same conditions, (c) relative difference between effective and lattice temperatures, (d) the calculated distribution function at $T_{\text{lat}} = 20$ K and $T_{\text{lat}} = 40$ K in a wider energy window. Dashed lines: distributions for $T_{\text{eff}} = 21$ K (blue) and $T_{\text{eff}} = 42$ K (black).

δ is essentially phonon assisted (both optical and acoustic), which agrees with the picture of an equilibrium phase transition. These results are consistent with the simulation performed in Refs. [14,15], where the polariton condensation assisted by acoustic phonons only was found possible under positive δ . One should note that the fit of the distribution function is not precise above threshold, first because interactions should introduce deviations from the Bose distribution, and also because the real polariton system is perturbed by structural disorder [8,9,16]. Figure 1(d) shows the calculated distribution functions on a wider energy range for $T_{\text{lat}} = 20$ K and $T_{\text{lat}} = 40$ K. It can be seen that most exciton polaritons follow a Bose distribution with a T_{eff} very close to T_{lat} : $T_{\text{eff}} = 21$ K for polaritons between 5 and 20 meV at $T_{\text{lat}} = 20$ K, and $T_{\text{eff}} = 42$ K for polaritons between 5 and 35 meV at $T_{\text{lat}} = 40$ K (solid and dashed lines are undistinguishable in these ranges). For polaritons at lower energy and accessible experimentally (0–4 meV), the T_{eff} is slightly smaller. Concerning the high energy part of the calculated distribution, the T_{eff} , of the order of 250 K, is mainly determined by the pumping term P_k . The number of these particles is, however, small and of little influence on the overall dynamics of the system.

Figure 2 shows the evolution of the measured (black points) and calculated (black line) P_{th} as a function of T_{lat} for $\delta \simeq +6$ meV. These results are compared with the critical densities n_c of the BEC obtained in the thermodynamic limit (red line) [2,16]. The density of particles for each P_{th} is obtained from kinetic simulations. This figure confirms the conclusions extracted from the effective temperature measurements. The P_{th} measured is a result of the balance between the relaxation kinetics, whose efficiency increases versus T_{lat} and the thermodynamic value of n_c which is increasing versus T_{lat} . In our case the threshold is always increasing versus T_{lat} , in agreement with a thermodynamic phase transition. One can, moreover, observe that the difference between the measured (calculated) P_{th} and the thermodynamic value is almost vanishing above $T_{\text{lat}} = 30$ K. This is in a full agreement with the effective temperature measurements and again with the picture of a BEC

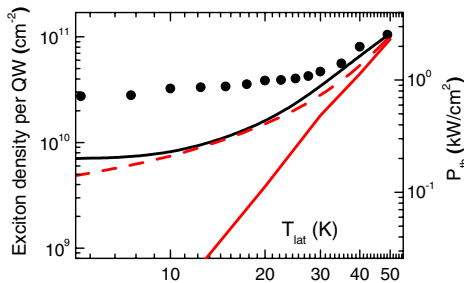


FIG. 2 (color online). Experimental (black circles) and calculated (black line) pumping threshold versus the lattice temperature at $\delta = +6$ meV. The red line shows the critical density for the polariton BEC, calculated in the thermodynamic limit (infinite particle lifetime). The red dashed line shows the thermodynamic density calculated using T_{eff} instead of T_{lat} .

at thermal equilibrium. The red dashed line shows the values of the thermodynamic threshold calculated using not T_{lat} , but T_{eff} . One can observe now a good agreement between the kinetic and thermodynamic curves, which confirms the observation of a phase transition occurring close of the thermodynamic equilibrium.

We now turn to measurements performed for $\delta = -1$ meV [see Fig. 3(a)]. In that case, polaritons close to the ground state are becoming $\sim 40\%$ more photonlike. Their lifetime is shorter and the dispersion around the ground state is steeper. All this makes polariton relaxation less efficient. On the other hand, the thermodynamic value of n_c is smaller because of the smaller effective mass. Figure 3(b) shows the measured occupancy versus the emission energy, for different P_{ext} at $T_{\text{lat}} = 5.2$ K. Figure 3(c) shows the corresponding simulations. For the lower powers these distributions cannot be described by an effective temperature, and a pronounced bottleneck effect can be observed [8,17]. When the condensation threshold is passed, the system evolves from a metastable state towards a condensed state. The distribution function at threshold is not yet thermal, but it evolves rapidly and a full equilibration is achieved and locked at around $5P_{\text{th}}$. This behavior is qualitatively well described by the calculations. We find at this δ , a dominant role of the exciton-polariton scattering processes, which are becoming stimulated above threshold, allowing to overcome the kinetic barrier. The results of our simulation at $\delta = -1$ meV are in qualitative agreement with the one of Ref. [13], where the exciton-polariton scattering was the only process that efficiently injects polaritons toward the lowest energy states.

Measurements and theoretical simulations of P_{th} as a function of δ at $T_{\text{lat}} = 5.4$ K and $T_{\text{lat}} = 25$ K are displayed in Figs. 4(a) and 4(b), respectively. In principle, the relaxation kinetics gets more efficient with increasing δ , owing to the increased rate of the phonon scattering. On the opposite, the thermodynamic threshold grows when increasing

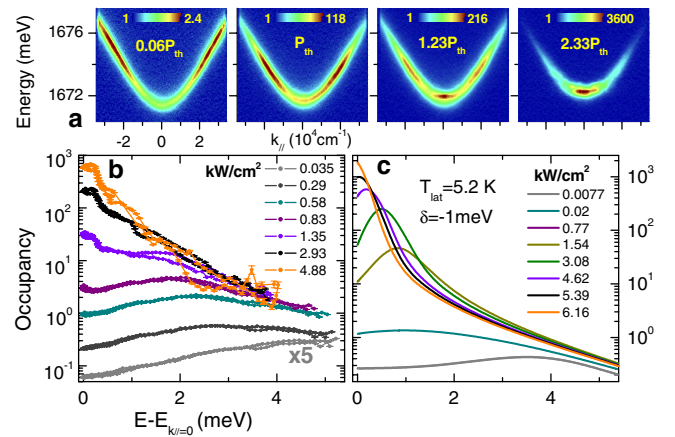


FIG. 3 (color online). (a) Spectrally resolved far-field polariton emission as a function of P_{ext} at $T_{\text{lat}} = 5.2$ K and for detuning $\delta = -1$ meV $= -0.038 \Omega$, logarithmic color scale; (b) experimental and (c) calculated distribution functions for different P_{ext} .

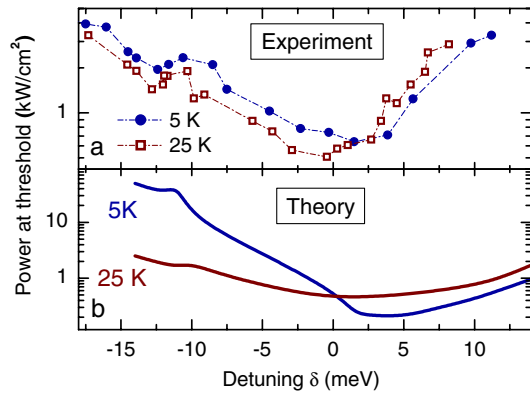


FIG. 4 (color online). (a) Measured P_{th} as a function of δ at $T_{lat} = 5$ K (solid blue circles) and $T_{lat} = 25$ K (open brown squares), (b) corresponding simulation.

δ , because of the increase of the polariton effective mass. The actual threshold which results from these two contradictory tendencies, should therefore first decrease at negative δ , when the kinetics is the limiting factor, then pass a minimum, where both kinetics and thermodynamics are playing an equivalent role, to finally increase in the δ positive region, where the phase transition is driven thermodynamically. One can observe a small minimum, or rather a change of slope, on the curve for $\delta \approx -13$ meV. At this δ , the transition between the exciton reservoir and the polariton ground state is resonant with the optical phonon energy [18]. Let us now compare the curves obtained at different T_{lat} . The kinetics is faster at $T_{lat} = 25$ K than at $T_{lat} = 5.4$ K. As a result, under negative δ , P_{th} is lower at 25 K with respect to 5.4 K, as shown by the data. In the thermodynamic regime the situation is inverted, because the thermodynamic threshold is lower at 5.4 K than at 25 K. The optimum threshold occurs, as it should be for a lower δ at 25 K with respect to 5.4 K. The qualitative agreement between experiment and simulation is quite satisfactory when considering that structural disorder is neglected in the simulation.

This whole set of results is summarized on the sketch shown in Fig. 5. We distinguish four phases which are (i) condensed phase in thermal equilibrium, (ii) uncondensed phase in thermal equilibrium, (iii) condensed metastable phase, and (iv) uncondensed metastable phase. There is no abrupt transition between a state in self-equilibrium ($T_{eff} \neq T_{lat}$) and a state in equilibrium with the lattice ($T_{eff} = T_{lat}$), so we did not consider them as belonging to different phases. The boundary between (i) and (iii) occurs at lower detuning and lower temperature with respect to the one between (ii) and (iv) because the relaxation kinetics is faster in the condensed phases with respect to the normal ones. All the transitions from an uncondensed to a condensed phase can be called polariton laser effects, because they exhibit a threshold for a coherent emission, driven by the accumulation of polaritons in their ground state. The condensation taking place between two metastable phases (arrow 1) can hardly be related with

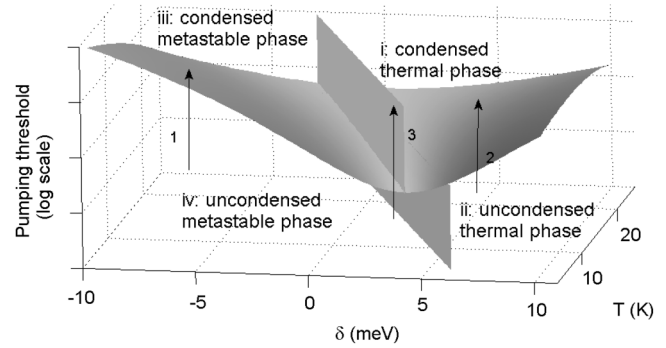


FIG. 5. Sketch of the polariton phase diagram (δ , T_{lat} , P_{th}) in the microcavity investigated. The surfaces symbolize the limits between the four possible phases. The arrows show the three possible types of condensation that can occur with increasing the pumping and keeping δ and T_{lat} constant.

the BEC, defined as an equilibrium phase transition. This situation occurs in our sample under negative δ and is favored by a small T_{lat} . On the other hand, the transition from an equilibrium uncondensed phase to an equilibrium condensed phase (arrow 2) shows the textbook features of the BEC defined as a thermodynamic phase transition. This situation occurs for positive δ and is favored by an increase of T_{lat} . Finally a third case occurs (arrow 3), when the transition takes place between the metastable uncondensed state and the equilibrium condensed state. This situation occurs in our sample for $\delta \approx 0$ meV. We propose to call this intermediate case *kinetically driven Bose condensation* because the final state is the state which should be reached by the system at thermal equilibrium.

We acknowledge support by the: EU Network HPRN-CT-2002-00298 “Photon-mediated phenomena in semiconductor nanostructures,” EU “STIMSCAT” N517769 and UK EPSRC Grant No. EP/D025303/1.

- [1] C. Weisbuch *et al.*, Phys. Rev. Lett. **69**, 3314 (1992).
- [2] A. Kavokin and G. Malpuech, *Cavity Polaritons* (Elsevier Academic Press, Amsterdam, 2003).
- [3] A. Imamoğlu *et al.*, Phys. Rev. A **53**, 4250 (1996).
- [4] G. Malpuech *et al.*, Appl. Phys. Lett. **81**, 412 (2002).
- [5] S. Chrisopoulos *et al.*, Phys. Rev. Lett. **98**, 126405 (2007).
- [6] L. V. Butov, Nature (London) **447**, 540 (2007).
- [7] D. Bajoni *et al.*, Phys. Rev. Lett. **100**, 047401 (2008).
- [8] M. Richard *et al.*, Phys. Rev. B **72**, 201301(R) (2005).
- [9] J. Kasprzak *et al.*, Nature (London) **443**, 409 (2006).
- [10] H. Deng *et al.*, Phys. Rev. Lett. **97**, 146402 (2006).
- [11] R. Balili *et al.*, Science **316**, 1007 (2007).
- [12] G. Malpuech *et al.*, Phys. Rev. B **65**, 153310 (2002).
- [13] D. Porras *et al.*, Phys. Rev. B **66**, 085304 (2002).
- [14] H. T. Cao *et al.*, Phys. Rev. B **69**, 245325 (2004).
- [15] T. Doan *et al.*, Solid State Commun. **145**, 48 (2008).
- [16] G. Malpuech *et al.*, Phys. Rev. Lett. **98**, 206402 (2007).
- [17] F. Tassone *et al.*, Phys. Rev. B **56**, 7554 (1997).
- [18] F. Bœuf *et al.*, Phys. Rev. B **62**, R2279 (2000).